J. Neurovirol. (2012) 18:462–470
DOI 10.1007/s13365-012-0124-z

Retrograde axonal transport of VZV: kinetic studies in hESC-derived neurons

Sergei Grigoryan · Paul R. Kinchington · In Hong Yang · Anca Selariu · Hua Zhu · Michael Yee · Ronald S. Goldstein

Received: 11 May 2012 / Revised: 30 July 2012 / Accepted: 31 July 2012 / Published online: 24 August 2012

Abstract Retrograde axonal transport of the neurotropic alphaherpesvirus Varicella zoster virus (VZV) from vesicles at the skin results in sensory neuron infection and establishment of latency. Reactivation from latency leads to painful herpes zoster. The lack of a suitable animal model of these processes for the highly human-restricted VZV has resulted in a dearth of knowledge regarding the axonal transport of VZV. We recently demonstrated VZV infection of distal axons, leading to subsequent capsid transport to the neuronal somata, and replication and release of infectious virus using a new model based on neurons derived from human embryonic stem cells (hESC). In the present study, we perform a kinetic analysis of the retrograde transport of green fluorescent protein-tagged ORF23 in VZV capsids using hESC-derived neurons compartmentalized microfluidic chambers and time-lapse video microscopy. The motion of the VZV was discontinuous, showing net retrograde movement with numerous short pauses and reversals in direction. Velocities measured were higher 1 h after infection than 6 h after infection, while run lengths were similar at both time points. The hESC-derived neuron model was also used to show that reduced neuronal spread by a VZV loss-of-function mutant for ORF7 is not due to the prevention of axonal infection and transport of the virus to the neuronal somata. hESC-derived neurons are, therefore, a powerful model for studying axonal transport of VZV and molecular characteristics of neuronal infection.

Keywords Axonal transport · Varicella zoster virus · Alphaherpesvirus · Human embryonic stem cells

Electronic supplementary material The online version of this article (doi:10.1007/s13365-012-0124-z) contains supplementary material, which is available to authorized users.

S. Grigoryan · R. S. Goldstein (✉)
Mina and Everard Goodman Faculty of Life Sciences,
Bar-Ilan University,
Gonda Building, Old Campus,
52900, Ramat-Gan, Israel
e-mail: ron.goldstein@biu.ac.il

P. R. Kinchington · M. Yee
Department of Ophthalmology,
University of Pittsburgh,
1020 EEI 203 Lothrop Street,
Pittsburgh, PA 15213, USA

P. R. Kinchington
Department of Microbiology and Molecular Genetics,
University of Pittsburgh,
1020 EEI 203 Lothrop Street,
Pittsburgh, PA 15213, USA

I. H. Yang
Department of Biomedical Engineering, School of Medicine,
Johns Hopkins University,
720 Rutland Avenue Traylor #715,
Baltimore, MD 21205, USA

I. H. Yang
SiNAPSE,
National University of Singapore,
Singapore, Singapore

A. Selariu · H. Zhu
Department of Microbiology and Molecular Genetics,
UMDNJ—New Jersey Medical School,
225 Warren Street,
Newark, NJ 07101-1709, USA

Introduction

Varicella zoster virus (VZV) belongs to the alphaherpesvirus family and like other members is neurotropic. Initial VZV infection results in varicella (chicken pox), in which characteristic virus-filled vesicles in the skin follow a systemic spread. VZV is then delivered to neuronal nuclei in ganglia by two

mechanisms, either via infected circulating immune cells (Ouwendijk et al. 2012) or by retrograde transport in axons infiltrating skin at sites of replication (reviewed in Zerboni and Arvin 2008). Neuronal infection becomes persistent through the establishment of latency, and subsequent reactivation usually leads to anterograde axonal transport to the periphery and the formation of lesions typical of herpes zoster (shingles), usually in older or immunocompromised persons. Unlike the related alphaherpesviruses pseudorabies virus (PrV) and herpes simplex viruses (HSV) whose wider host range has facilitated study in animal systems, VZV is highly human-tropic: infection of most animal neurons does not result to a full productive infection (Steain et al. 2010). There have been a few studies of VZV infection of isolated human fetal dorsal root ganglion (DRG) neurons; however, the limited accessibility to this material has resulted in the direct demonstration of axonal transport and retrograde infection of neurons by VZV being performed only very recently by our groups (Markus et al. 2011).

Elegant and extensive work with HSV-1 and PrV has shown that these two alphaherpesviruses are stripped of their external glycoprotein-containing envelope and of many tegument proteins when they infect axons (Luxton et al. 2005; Antinone et al. 2006 reviewed in Diefenbach et al. 2008). The DNA-containing nucleocapsid with some inner tegument proteins is then transported retrogradely to the neuronal nucleus, where a latent or productive infection ensues. Retrograde axoplasmic transport using the dynein motor protein complex is responsible for bringing chemical messages, endocytosed material and cellular components for recycling from the axon terminals back to the cell body. Anterograde axoplasmic transport utilizes instead kinesin motor proteins and delivers vesicles, proteins and other structural cellular materials from the somata towards the periphery (reviewed in, i.e., Goldstein and Yang 2000; Hirokawa and Takemura 2005). Both HSV and PrV co-opt the extant retrograde and anterograde axonal transport processes in order to travel from the periphery to the soma (in initial infection) or from the soma to the periphery (in reactivation), respectively (reviewed in Diefenbach et al. 2008; Lyman and Enquist 2009; Zaichick et al. 2011). Studies of HSV and PrV transport by video time-lapse micrography, using avian and rodent DRG neurons as well as human neuron-like cells derived from a cancer cell line, show that both retrogradely and anterogradely transported viruses/capsids move discontinuously and even reverse direction (Smith et al. 2004; Antinone and Smith 2010). Using genetically modified viruses expressing fluorescent proteins, a great deal has been learned about which viral proteins interact with the cellular machinery, but a final detailed model is yet to be generated. It is not yet known which, if any, of these parameters extend to the axonal transport of VZV, largely because of the lack of an animal model that accurately recapitulates VZV infection and replication in neurons.

Human embryonic stem cells (hESC) have been shown to differentiate into neurons that are useful for studying various aspects of neuronal cell biology, including disease mechanisms (reviewed in Friedrich Ben-Nun and Benvenisty 2006) and axonal regeneration after injury (Ziegler et al. 2010). Our group has recently shown that these hESC-derived neurons can be efficiently infected by VZV in vitro, leading to a productive replication and subsequent infection of neighboring cells (Markus et al. 2011). Furthermore, we used compartmentalized microfluidic chambers, similar to those used by others for studying PrV transport (Liu et al. 2008), to demonstrate the peripheral axonal infection of neurons and that VZV undergoes retrograde axonal transport to initiate infection of human neurons.

In the present study, we extend our analyses of VZV retrograde transport in hESC-derived neurons using genetically modified viruses, microfluidic chambers and time-lapse microscopy. Using VZV tagged with green fluorescent protein (GFP) on a capsid protein, we performed a kinetic analysis of retrogradely moving viral particles inside axons. In addition, we examined whether a VZV protein recently shown to be important in neurotropism, ORF7 (Selariu et al. 2012), is required for the transport of capsids from axons to the neuronal nuclei.

Methods

Generation of human neurospheres and neurons

Neurons were differentiated from hESC-derived neural precursor-containing aggregates (neurospheres) generated by coculturing hESC with the PA6 mouse stromal cell line in a method similar to that previously described (Pomp et al. 2008; Markus et al. 2011). About 6×10^4 hESC were plated in a 10-cm culture dish containing a monolayer of PA6 cells in 90 % BHK-21 medium/Glasgow minimal essential medium, 10 % knockout serum replacement, 2 mM glutamine, 1 mM sodium pyruvate, 0.1 mM nonessential amino acid and 0.1 mM β-mercaptoethanol. The coculture was incubated for 2 weeks and the medium was changed every 2 days. At days 12–14, colonies with a homogeneous morphology were manually cut from the plate (Pomp et al. 2008) and transferred to microfluidic chambers. Terminal differentiation was obtained in neural induction medium (NIM; Dulbecco's modified Eagle's medium/nutrient mixture F-12, 1 mM glutamine, 50 U/ml penicillin, 50 μg/ml streptomycin, B27 supplement (1:50), 10 ng/ml nerve growth factor (NGF), 5 ng/ml brain-derived neurotrophic factor (BDNF), and 10 ng/ml NT3) which was changed three times a week. This protocol differs from that we have used in the past in that the neurospheres were plated on laminin for terminal differentiation without initial culture in suspension. The neuronal cultures prepared with this method contain more than 90 % neurofilament-M immunopositive neurons (Reis et al., manuscript in preparation).

Culture and axonal infection of hESC-derived neurons in compartmented microfluidic chambers

Microfluidic chambers with two compartments connected by microchannels (length, 450 μm; height, 3 μm; width, 10 μm) were prepared as previously described (Yang et al. 2009). The chambers were sterilized with 70 % ethanol, coated with poly-L-lysine/laminin, and hESC-derived neurospheres were plated adjacent to the microchannels in NIM in one compartment ("cell body compartment"). The axonal compartment contained the same medium with a 10-fold higher NGF concentration for attracting axons (Campenot 1977). The media were changed three times a week. Axons grew from the cell body compartment to the axonal compartment through the microchannels within 3–4 days. The processes were axons, based on their being over 450 mm in length, and immunopositive for the axonal protein Tau (not shown). After an extensive plexus of axons had formed in the axonal chamber (approximately 1 week after the first axons reached the compartment), 10^5 VZV-infected MeWo or ARPE-19 cells were seeded on the axons in NIM. A volume gradient of medium was established between the two compartments, blocking the ability of free VZV to migrate through the microchannels (Taylor et al. 2005; Markus et al. 2011).

Recombinant VZV expressing GFP

A recombinant VZV derived from the parent Oka strain with GFP fused to the N-terminal end of the abundant capsid protein ORF23 (VZV-GFP23) was constructed using the VZV bacterial artificial chromosome (BAC) (Erazo et al. 2008) and has been detailed previously (Markus et al. 2011). This virus allows visualization of capsids/virions in neurons (Markus et al. 2011). Sucrose gradient fractionation and Western blotting show that type A (empty), B (closed, non-DNA containing), and C (DNA containing) capsids are labeled by GFP (Supplementary data 1). A virus containing a full deletion mutant of the ORF7 gene (VZV-7D) and driving GFP expression under an SV40 promoter was generated as described in Zhang et al. (2010). VZV was maintained in MeWo or ARPE19 cells.

Microscopic imaging

Live cultures were viewed and photographed with an Olympus IX70 inverted microscope using a Jenoptiks ProgRes CF^{cool} digital camera (Jena, Germany). Movies, mostly <30 s, but some up to 2.5 min, were obtained with a Zeiss Observer.Z1 using an Plan Apochromat ×100/1.4 NA oil objective and AxioCam HSm or Hamamatsu digital cameras. A Lambda DG-4 light source with an integrated filter changer or a Nikon Intensilight was used for fluorescence illumination. Fluorescence images were taken with exposures of 500–800 ms, the fastest image capture rate our system allows. During acquisition of the movies, cultures were maintained in 5 % CO_2, 37 °C and 95 % humidity. Zeiss Axiovision and Jenoptiks software were used for recording movies and images, respectively. Differential interference contrast (DIC) images were collected at the end of the movies.

Kinetic analysis

Movies were analyzed using the SpotTracker2D (http://bigwww.epfl.ch/sage/soft/spottracker/gasser.html) plug-in for ImageJ (http://rsbweb.nih.gov/ij/). The SpotEnhancing Filter2D was applied before the analysis in order to enhance the contrast and simplify following the capsids. Kinetic parameters were calculated from the plug-in output using Microsoft Excel, and curve fitting and statistical analysis was performed with SPSS. Movements of <2–3 pixels were considered "pauses" for dividing movies into "runs" (i.e., Antinone and Smith 2010).

Results

Retrograde axonal transport of VZV from axons to cell bodies in compartmentalized microfluidic chambers

Our recent study of the infection of hESC-derived neurons by VZV demonstrated that retrograde transport of VZV occurs in these cells (Markus et al. 2011). Using the same experimental platform (hESC-derived neurons grown in compartmented microfluidic chambers in combination with VZV containing GFP fused to the ORF23 capsid protein (VZV-GFP23)), we now examined this transport with live fluorescence microscopy. hESC-derived neuronal precursors were seeded in the cell body compartments of microfluidic chambers, and after differentiation to neurons, extended their axons through microchannels to the axonal compartments. VZV-GFP23-infected MeWo or ARPE cells were then added to the axonal compartments. One hour or 6 h after the addition of the VZV-infected input cells, the living cultures were examined with video microscopy. Many GFP-fluorescent dots were observed in the human axons adjacent to microchannels in the axonal compartment (Fig. 1a). These dots are likely to be single VZV-GFP23 capsids, based on studies of PrV and HSV-1 transport (Smith et al. 2001) and the uniformity of the GFP signals. GFP-fluorescent capsids were also observed inside the axons throughout the microchannels (Fig. 1b) and inside axons close to the cell body compartments (Fig. 1c and inset) 6 to 10 h after the addition of the MeWo cells. Recording a series of fluorescence images showed that the capsids were in motion within the axons inside the

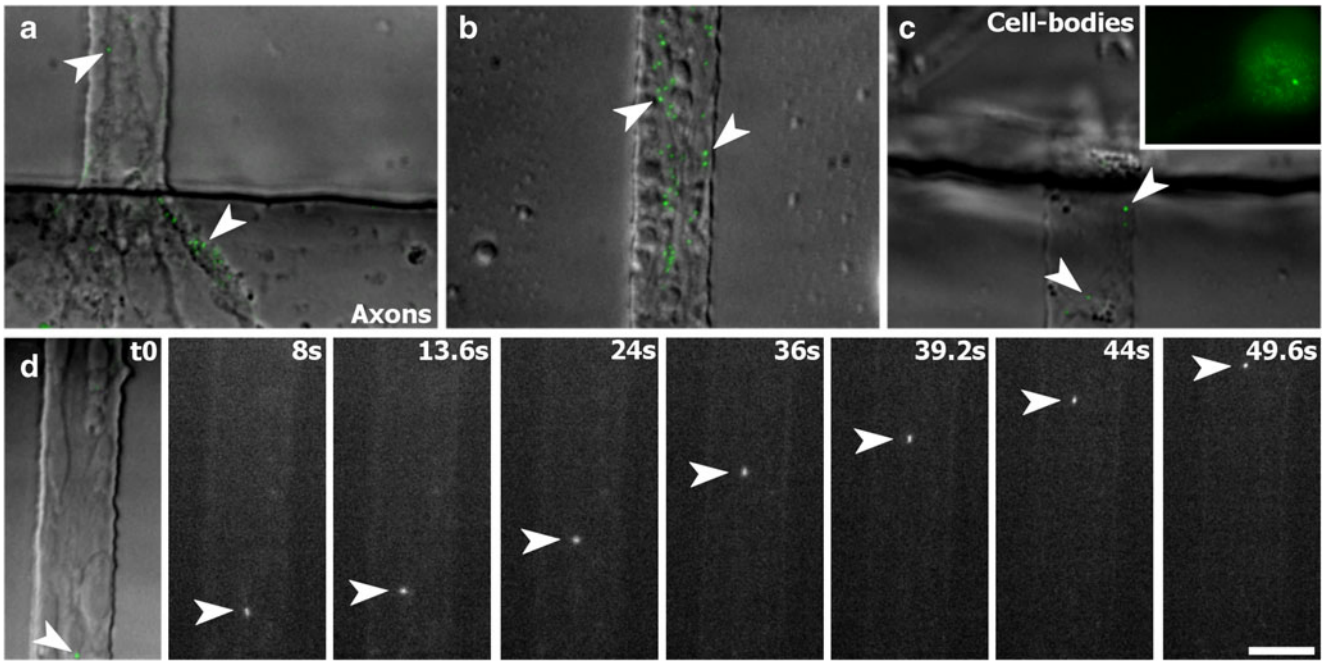

Fig. 1 Retrograde axonal transport of VZV capsids between compartmentalized microfluidic chambers. hESC-derived neurons were seeded and grown in the "soma" compartments of microfluidic chambers and, after several days, extended axons into the "axonal" compartments (*lower part* of **a**). MeWo cells infected with VZV-GFP23 were then added to the axonal compartment. **a** GFP-fluorescent capsids (i.e., at *arrowheads*) inside axons adjacent to a microchannel in the axonal compartment 6 h after the initial infection. **b** Capsids within microchannels. **c** Fluorescent capsids inside axons entering the cell body compartment (*top*). The *inset* shows a GFP-fluorescent soma 24 h PI. **d** Individual frames from a movie of a single retrogradely moving GFP-tagged capsid inside a microchannel over a period of 50 s. **a**–**d** first panel, combined fluorescence and DIC (Nomarski) images. Scale bar for all images, 10 μm

microchannels. Selected frames from a time series following an individual capsid shown in Fig. 1d show directed movement towards the soma side of the chambers.

Kinetics of VZV-GFP23 particle movement in axons

In order to characterize the nature of transport and to obtain estimates of retrograde transport velocity, live monitoring of individual GFP-fluorescent particles was used to obtain time-lapse movies at rates of 1.25–2 frames per second within the microchannels 1–6 h after infection (Supplementary data 2 and 3). While most of the GFP-positive dots in the channels did not show directed motion during the time period of observation (as observed for PrV and HSV; Smith et al. 2001; Antinone and Smith 2010), many particles progressed in a retrograde direction. Thirty-seven particles were followed for periods ranging between several seconds and 2.5 min (Table 1). Motion of the VZV capsids was not continuous or always in the retrograde direction. Many pauses in particle movement and reversals in direction were observed. The kinetics of the nucleocapsid movement was then analyzed using a movement-tracking plug-in for the image processing program, ImageJ (Fig. 2a, c; see the "Methods" section). Data from movies collected 1 h after seeding of input cells (postinfection [PI]) were analyzed separately from those collected 6–10 h PI. The instantaneous velocity and direction of movement between frames of the movie were measured and graphed against time (Fig. 2b, d).

Table 1 Kinetic analysis of retrograde transport of VZV capsids in human axons

Time after infection (h)	Capsids analyzed	Runs	Average retrograde velocity/run (μm/s)	Maximal instantaneous velocity/run (μm/s)	Average run length (μm)
1	27	93	1.35±0.63	5.3	3.8
6–10	10	56	1.07±0.54	4.4	3.5

Movies of VZV capsids were obtained and kinetic analysis was performed as described in the "Methods" section. The table shows the numbers of capsids and runs analyzed, as well as the values obtained for average and maximal velocity and average run length of capsids observed at 1 and 6–10 h PI

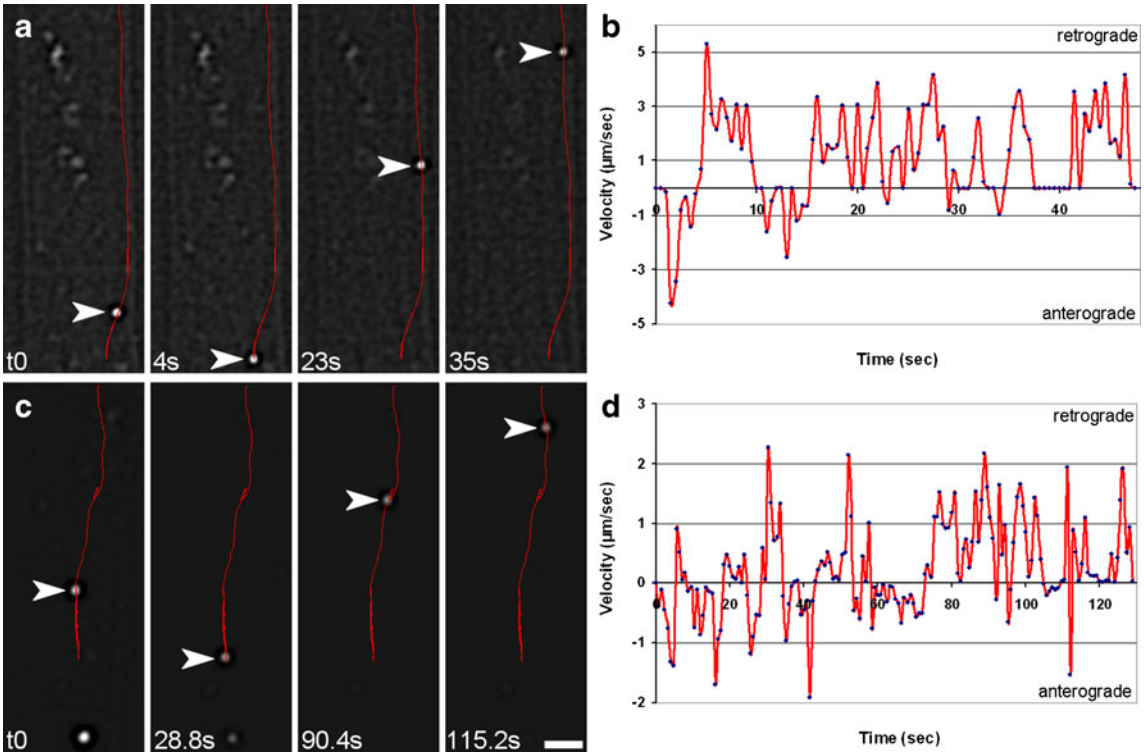

Fig. 2 Tracking of VZV capsid transport in human axons. Individual GFP-fluorescent capsids imaged in microchannels 1 h (**a**, **b**) and 6 h (**c**, **d**) after the addition of VZV-infected MeWo cells to the axonal compartment. **a**, **c** Frames from movies of individual moving capsids (*arrowheads*) that were captured at a frequency of 1.25–2 frames per second. The *red line* is the output of the ImageJ SpotTracker plug-in that traces the course of the capsid in the axon. Movements toward the cell bodies (retrograde) are shown as positive values, and movements back toward the axonal chamber (anterograde) are negative values (**b**, **d**) Plots of the instantaneous velocities of capsids. Both capsids showed many short reversals in direction in addition to a few pauses in motion. Scale bars in **a**, **c**, 5 μm

The kinetics of PrV and HSV axonal transport has been performed by collecting data from "runs" in which capsids/viruses were moving continually about 1 h PI (Antinone and Smith 2010). In order to obtain values for velocity comparable to those obtained in previous studies, the movies were divided into runs by pauses (movements of <2–3 pixels) or reversals in direction. The retrograde velocities for over 90 runs from 27 capsids was found to average about 1.4 μm/s, and the distribution was approximately Gaussian (normal distribution according to one-sample Kolmogorov–Smirnov test; Fig. 3a). The maximal instantaneous velocity of retrograde motion observed was 5.3 μm/s. We also collected data for the lengths of the runs and plotted them and found that they could be described by an exponential decay (r^2=0.968) (Fig. 3c), as described for PrV and HSV-1.

It has been reported that the number of stalled capsids increases in frequency with time after infection (Smith et al. 2001). In order to see if the kinetics of those capsids still being transported was changed at later times PI, we repeated our experiments at 6 h PI and compared the average velocities and run lengths of capsids obtained at early and later times PI. Subjectively, it was clear that many fewer capsids were in motion in the axons at the later time point. Analysis of 56 runs from 10 capsids obtained at 6 h PI revealed that transport was significantly slower than at 1 h PI (1.1 vs. 1.4 μm/s, p<0.01; Fig. 3b), and the maximal velocity was also slower (4.4 vs. 5.3). The distribution of average particle velocities was again consistent with a normal distribution. Analysis of run length distributions at 6 h PI showed an exponential decay (r^2=0.980; Fig. 3d), as was observed at 1 h PI. The results of the kinetic analyses are summarized in Table 1.

Use of hESC-derived neurons in microfluidic chambers as an aid to understanding viral gene function

A study creating loss-of-function mutations in all of the VZV ORFs revealed that the deletion of ORF7, a nonessential VZV gene, negatively affected the spread of infection in skin organ culture (Zhang et al. 2010). More recently, ORF7 has been determined to be important for neuronal infection as well (Selariu et al. 2012). We, therefore, used the microfluidic chamber hESC-derived neuron experimental platform to address the question of ORF7's role in VZV axonal infection and transport. ARPE19 cells infected with the ORF7 deletion mutant (VZV-7D) or the parental strain

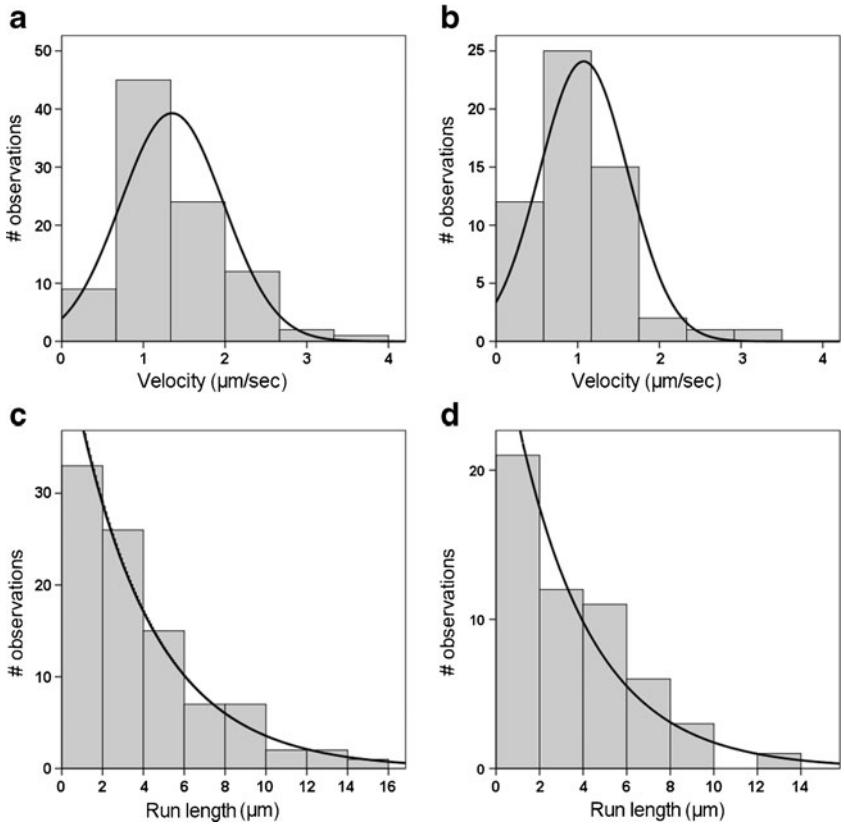

Fig. 3 Kinetic analysis of VZV capsid movement in human axons. **a**, **b** The distribution of average velocities of runs of retrograde VZV capsid motion obtained from live imaging of axons of hESC-derived neurons in microfluidic channels at 1 and 6–10 h PI, respectively. The average velocity at 1 h PI was moderately but significantly higher than at the later times PI, see Table 1 for values and the text for discussion. The distributions are apparently unimodal and normal, and Gaussian curves are superimposed on the graphs. **c**, **d** The distribution of run lengths of VZV capsids moving retrogradely observed 1 and 6–10 h PI. Run lengths decay exponentially at both early and later times PI

(VZV-$_{BAC}$), (Zhang et al. 2008) were seeded with axons of hESC-derived neurons. Both of these viruses express GFP under the control of a SV40 promoter. Three days after seeding on the axons, similar amounts of neuronal cell bodies were GFP-fluorescent in cell body compartments containing both infecting viruses (Fig. 4a, d). After an additional 3 days in culture, the cell body compartments of chambers whose axons were infected with VZV-7D contained additional fluorescent cell bodies (Fig. 4e, f), although the collections of fluorescent somata were much less dense than those observed after infection with the WT-VZV-$_{BAC}$ virus (Fig. 4b, c). Similar results were obtained in six pairs of control WT and VZV-7D infected compartmented chambers in four independent experiments. Since the initial amount of retrogradely infected neurons appeared similar for WT and mutant viruses, these results strongly suggest that deletion of ORF7 does not affect the entrance of VZV into axons or transport of VZV capsids to the nucleus and is consistent with the previously demonstrated reduction of spread between neurons and skin cells (Zhang et al. 2010; Selariu et al. 2012).

We also obtained evidence consistent with the recently demonstrated role of ORF7 in neuron to neuron spread in one of the microfluidic chamber experiments described above. In this experiment, after observing the first GFP-positive somata of both VZV-7D- and WT-VZV-$_{BAC}$-infected neurons, the axons and VZV-infected input cells were removed from the axonal compartment, thus preventing additional neurons from being infected in the cell body compartment by newly generated and transported virus. After an additional 3 days of incubation, almost no new GFP-fluorescent cell bodies had appeared in the chambers infected with VZV-7D, while a large increase in the number of cell bodies expressing GFP was observed in the chamber infected with WT-VZV (not shown), confirming observations using hESC-derived neurons and human fetal neurons in conventional tissue culture (Selariu et al. 2012).

Discussion

We recently demonstrated distal axonal VZV infection and retrograde transport that leads to productive infection in hESC-derived neurons (Markus et al. 2011). These observations are expanded in the current study by obtaining kinetic data for VZV movement in retrograde transport and demonstrate that hESC-derived neurons can be used to study VZV protein function in neurons. Alphaherpesvirus transport of PrV and HSV have been studied in neuron-like cells derived from neuroblastoma (Antinone and Smith 2010). However, our study is the first using neurons derived from genetically normal human stem cells that have been shown to (1) have bona fide axons expressing TAU (Ziegler et al. 2010 and not shown), (2) make neurotransmitters, and (3) have electrophysiological properties of neurons (i.e.,

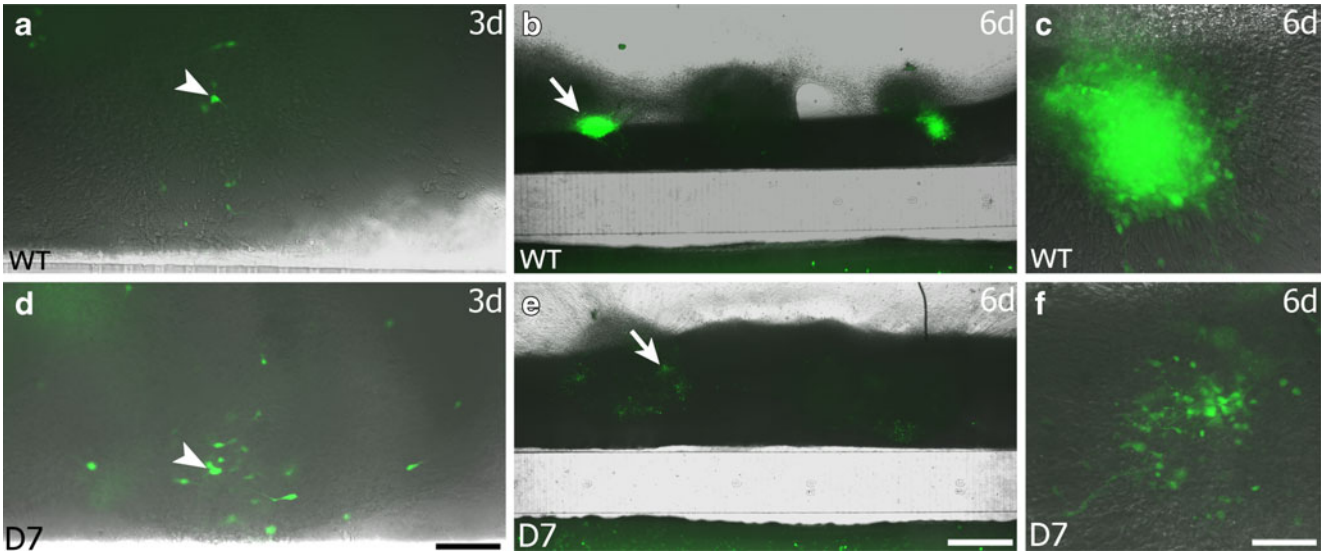

Fig. 4 Deletion of VZV ORF7 does not prevent axonal infection or retrograde transport of capsids. Axons of hESC-derived neurons grown in microfluidic chambers were infected with WT VZV-$_{BAC}$ (**a**–**c**) or a virus containing a deletion for ORF7 (VZV-7D) (**d**–**f**). Both viruses produce GFP under the control of an independent SV40 promoter (**a**). Retrogradely infected neurons were observed in the cell body compartment 3 days after infection with the WT virus. The *arrowhead* points to a neuron with both soma and axon filled with GFP. **b** The same compartment 6 days PI (3 days after the image shown in **a**). Two foci of GFP-positive neurons (i.e., at the *arrow*) are now seen (note the much lower magnification in **b** than in **a**). **c** Higher magnification of right-hand cluster of infected neurons seen in **b** shows the high-density cluster of GFP-positive neurons and some individual GFP-positive neurons outside the cluster. **d** At 3 days PI, individual GFP-positive neurons were also observed in the cell body compartment after infection of their axons with mutant VZV-7D (**e**). Three days later (6 days PI), groups of GFP-positive somata but no clusters with a high-density of fluorescent neurons were observed, in contrast to the WT virus (**b**). **f** Higher magnification of a zone containing GFP-positive cells from the chamber in **e**, showing that the density of GFP-positive neurons is much lower than that observed in **c**. **a**, **c**, **d**, **f** are merged phase-contrast and fluorescence images and **b**, **e** only show GFP fluorescence. Scale bars of **a**, **c**, **d**, **f**, 100 μm; **b**, **e**, 500 μm

Pomp et al. 2008). This model permitted live-image VZV capsid movement for the first time and allowed comparison of the kinetics of VZV retrograde transport to the many studies of alphaherpesviruses with a greater host range such as PrV and HSV-1.

In most studies of PrV and HSV-1, chick or mouse DRG neurons were infected in conventional dissociated neuron cultures and motion was observed within the first 1 h or so after introduction of the virus. The analyses performed in those studies obtained values of transport rate in continuous runs of retrograde movement of capsids of approximately 1 μm/s (Smith et al. 2001) and 2 μm/s (Antinone and Smith 2010), with the speeds having a Gaussian distribution. In later studies, transport in human neuron-like cells differentiated from neuroblastoma was found to be similar to that in mouse and chick neurons under the same conditions, 2 μm/s. These studies also reported that most capsids observed were not in motion and that those that did move paused and reversed direction of movement. It is worthwhile to note that both VZV and HSV-1 are human pathogenic viruses, and there may be an advantage to study their transport in human neurons to more accurately understand human disease. It is quite possible that the human virus behavior/mechanisms of transport differ between human and animal neurons, as is the case for the replication of VZV, which does not occur in most non-human cultured cells.

The kinetic analysis we performed of VZV retrograde movement in human axons early after infection yielded an average velocity of about 1.4 μm/s during runs distributed in an apparently Gaussian manner. This is more than that observed for PrV retrograde axonal transport using microfluidic chambers (0.7 μm/s; Liu et al. 2008) and in one study of PrV in chick axons (1 μm/s) (Smith et al. 2001), but less than that observed more recently (Antinone and Smith 2010), as mentioned above. The differences may be due to a difference between VZV and the other alphaherpesviruses, to culture conditions, or to the differences between the neurons used in the studies, as suggested by others (Liu et al. 2008; Antinone and Smith 2010). In a preliminary experiment using HSV-mCherryVP26, HSV-1 capsids were observed to travel retrogradely at an average velocity of 1.3 μm/s, similar to the value we obtained for VZV. This suggests that the culture conditions or the types of neurons infected are responsible for the differences in transport speeds found in different studies and that different alphaherpesviruses are likely to travel at the same speed in neurons of the same type.

We performed observations of capsid transport both early after axonal infection and after it had proceeded for 6–10 h.

The average velocity of the capsids during runs was moderately but significantly reduced at later times, and the maximal velocity and average run lengths were also reduced. There are many potential explanations for these changes in capsid transport kinetics. For example, dynein can move both anterogradely and retrogradely, and the ratio between the directionalities can affect the overall velocity (Ross et al. 2006; Gross et al. 2000). Other possibilities include that the number of dynein motors available is reduced, changing velocity or direction of the movement (Hendricks et al. 2010; Schroeder et al. 2010), or there is a drop in the amount of available adenosine triphosphate for transport (perhaps also explaining the higher proportion of stationary capsids we and others observe). Future experiments of VZV or PrV/HSV transport using compartmented chambers at multiple time points with molecular/pharmacological perturbations may allow distinction between these different mechanisms and shed additional light on the retrograde transport of alphaherpesviruses.

Although there have been many studies of the roles of individual VZV proteins in infection/interaction of non-neuronal cells, much less is known for neurons. Since VZV remains latent in the nervous system and frequently reactivates to cause painful disease, an understanding of the molecular basis of VZV–neuron interactions has high significance. In a sweeping survey of the effects of mutating all the VZV ORFs, ORF7 was found to be a nonessential gene that, nevertheless, had an important role in skin tropism (Zhang et al. 2010). It has recently been shown that ORF7-deficient VZV have a reduced ability to spread in neurally differentiated neuroblastoma, human fetal DRG neurons, and hESC-derived neurons when added directly to the neuronal cells (Selariu et al. 2012). Using axonal infection in the hESC-derived neuron microfluidic chamber model, we show here that the lack of spread of infection between neurons is not due to (1) the inability of virus to infect axons and (2) the inability of capsids to be transported along axons to the nucleus, since somata of axonally infected VZV-7D express GFP. This experiment demonstrates that the hESC-derived neuron microfluidic chamber system permits the study of the viral genetics of neuronal infection and transport from axons by VZV. It is worthwhile to note that, in contrast to the primary neurons usually used in herpesvirus transport studies, hESC can be relatively easily modified genetically, allowing manipulation of the cellular transport machinery for future studies of the molecular basis of VZV transport.

Together, the results presented here establish that easily generated hESC-derived neurons grown in compartmented microfluidic chambers and infection by fluorescently tagged viruses are a powerful experimental system for exploring the biology of VZV interactions with neurons. We are currently using this system to examine the roles of individual VZV tegument proteins in retrograde transport. In light of the apparent differences between the viral proteins used by PrV and HSV for interacting with the dynein motor system (discussed by Antinone and Smith 2010), a study of those involved in VZV transport will also likely reveal differences from the other studied alphaherpesviruses. This powerful model can also be extended to study anterograde transport of and infection of target cells by VZV for a better understanding of processes occurring in zoster.

Acknowledgments This study was supported by Israel Science Foundation grant ##238/11 (RSG): NIH grants NS064022 and EY08098, and funds from the Research to Prevent Blindness Inc. and The Eye & Ear Foundation of Pittsburgh (PRK). Dr. Lina Gamarnik (Ziegler) performed preliminary experiments leading to the shortening of the protocol for neuron differentiation via PA6 cells. The authors thank Chaya Morgenstern and Michael Lee for the technical and logistic support and Dr. Rachel Levy-Drummer for the help with the statistics. Our gratitude to Dr. Mike Fainzilber for his insights on retrograde transport. Special thanks to Dr. Alexander Perelman for his personal guidance in live imaging experiments.

Conflict of interest No conflicts of interest are declared.

References

Antinone SE, Smith GA (2010) Retrograde axon transport of herpes simplex virus and pseudorabies virus: a live-cell comparative analysis. J Virol 84:1504–1512. doi:10.1128/JVI.02029-09

Antinone SE, Shubeita GT, Coller KE et al (2006) The herpesvirus capsid surface protein, VP26, and the majority of the tegument proteins are dispensable for capsid transport toward the nucleus. J Virol 80:5494–5498. doi:10.1128/JVI.00026-06

Campenot RB (1977) Local control of neurite development by nerve growth factor. Proc Natl Acad Sci USA 74:4516–4519

Diefenbach RJ, Miranda-Saksena M, Douglas MW, Cunningham AL (2008) Transport and egress of herpes simplex virus in neurons. Rev Med Virol 18:35–51. doi:10.1002/rmv.560

Erazo A, Yee MB, Osterrieder N, Kinchington PR (2008) Varicella-zoster virus open reading frame 66 protein kinase is required for efficient viral growth in primary human corneal stromal fibroblast cells. J Virol 82:7653–7665. doi:10.1128/JVI.00311-08

Friedrich Ben-Nun I, Benvenisty N (2006) Human embryonic stem cells as a cellular model for human disorders. Mol Cell Endocrinol 252:154–159

Goldstein LS, Yang Z (2000) Microtubule-based transport systems in neurons: the roles of kinesins and dyneins. Annu Rev Neurosci 23:39–71. doi:10.1146/annurev.neuro.23.1.39

Gross SP, Welte MA, Block SM, Wieschaus EF (2000) Dynein-mediated cargo transport in vivo. A switch controls travel distance. J Cell Biol 148:945–956

Hendricks AG, Perlson E, Ross JL et al (2010) Motor coordination via a tug-of-war mechanism drives bidirectional vesicle transport. Curr Biol 20:697–702. doi:10.1016/j.cub.2010.02.058

Hirokawa N, Takemura R (2005) Molecular motors and mechanisms of directional transport in neurons. Nat Rev Neurosci 6:201–214. doi:10.1038/nrn1624

Liu WW, Goodhouse J, Jeon NL, Enquist LW (2008) A microfluidic chamber for analysis of neuron-to-cell spread and axonal transport of an alpha-herpesvirus. PLoS One 3:e2382. doi:10.1371/journal.pone.0002382

Luxton GWG, Haverlock S, Coller KE et al (2005) Targeting of herpesvirus capsid transport in axons is coupled to association with specific sets of tegument proteins. Proc Natl Acad Sci USA 102:5832–5837. doi:10.1073/pnas.0500803102

Lyman MG, Enquist LW (2009) Herpesvirus interactions with the host cytoskeleton. J Virol 83:2058–2066. doi:10.1128/JVI.01718-08

Markus A, Grigoryan S, Sloutskin A et al (2011) Varicella-zoster virus (VZV) infection of neurons derived from human embryonic stem cells: direct demonstration of axonal infection, transport of VZV, and productive neuronal infection. J Virol 85:6220–6233. doi:10.1128/JVI.02396-10

Ouwendijk WJD, Mahalingam R, Traina-Dorge V et al (2012) Simian varicella virus infection of Chinese rhesus macaques produces ganglionic infection in the absence of rash. J Neurovirol 18:91–99. doi:10.1007/s13365-012-0083-4

Pomp O, Brokhman I, Ziegler L et al (2008) PA6-induced human embryonic stem cell-derived neurospheres: a new source of human peripheral sensory neurons and neural crest cells. Br Res 1230:50–60

Ross JL, Wallace K, Shuman H et al (2006) Processive bidirectional motion of dynein–dynactin complexes in vitro. Nat Cell Biol 8:562–570. doi:10.1038/ncb1421

Schroeder HW 3rd, Mitchell C, Shuman H et al (2010) Motor number controls cargo switching at actin-microtubule intersections in vitro. Curr Biol 20:687–696. doi:10.1016/j.cub.2010.03.024

Selariu A, Cheng T, Tang Q et al (2012) ORF7 of varicella zoster virus is a neurotropic factor. J Virol. doi:10.1128/JVI.00128-12

Smith GA, Gross SP, Enquist LW (2001) Herpesviruses use bidirectional fast-axonal transport to spread in sensory neurons. Proc Natl Acad Sci USA 98:3466–3470. doi:10.1073/pnas.061029798

Smith GA, Pomeranz L, Gross SP, Enquist LW (2004) Local modulation of plus-end transport targets herpesvirus entry and egress in sensory axons. Proc Nat Acad Sci USA 101:16034–16039. doi:10.1073/pnas.0404686101

Steain M, Slobedman B, Abendroth A (2010) Experimental models to study varicella-zoster virus infection of neurons. Curr Top Microbiol Immunol 342:211–228. doi:10.1007/82_2010_15

Taylor AM, Blurton-Jones M, Rhee SW et al (2005) A microfluidic culture platform for CNS axonal injury, regeneration and transport. Nat Methods 2:599–605

Yang IH, Siddique R, Hosmane S et al (2009) Compartmentalized microfluidic culture platform to study mechanism of paclitaxel-induced axonal degeneration. Exp Neurol 218:124–128

Zaichick SV, Bohannon KP, Smith GA (2011) Alphaherpesviruses and the cytoskeleton in neuronal infections. Viruses 3:941–981. doi:10.3390/v3070941

Zerboni L, Arvin AM (2008) The pathogenesis of varicella-zoster virus neurotropism and infection. Neurotropic viral infections. Cambridge University Press, Cambridge, pp 225–250

Zhang Z, Huang Y, Zhu H (2008) A highly efficient protocol of generating and analyzing VZV ORF deletion mutants based on a newly developed luciferase VZV BAC system. J Virol Methods 148:197–204. doi:10.1016/j.jviromet.2007.11.012

Zhang Z, Selariu A, Warden C et al (2010) Genome-wide mutagenesis reveals that ORF7 is a novel VZV skin-tropic factor. PLoS Pathog 6:e1000971. doi:10.1371/journal.ppat.1000971

Ziegler L, Segal-Ruder Y, Coppola G et al (2010) A human neuron injury model for molecular studies of axonal regeneration. Exp Neurol 223:119–127